Environmental Pollution 220 (2017) 766–778

Contents lists available at ScienceDirect

Environmental Pollution

journal homepage: www.elsevier.com/locate/envpol

Source apportionment of fine and coarse particles at a roadside and urban background site in London during the 2012 summer ClearfLo campaign☆

Leigh R. Crilley [a], Franco Lucarelli [b, c], William J. Bloss [a], Roy M. Harrison [a, *], David C. Beddows [a], Giulia Calzolai [c], Silvia Nava [b], Gianluigi Valli [d], Vera Bernardoni [d], Roberta Vecchi [d]

[a] School of Geography, Earth and Environmental Sciences, University of Birmingham, Edgbaston, Birmingham, B15 2TT, United Kingdom
[b] Dipartimento di Fisica e Astronomia, Università di Firenze, Via Sansone 1, 50019, Sesto Fiorentino, Firenze, Italy
[c] INFN, Sezione di Firenze, Via Bruno Rossi 1, 50019, Sesto Fiorentino, Firenze, Italy
[d] Department of Physics, Università degli Studi di Milano & INFN-Milan, Via Giovanni Celoria 16, 20133, Milan, Italy

ARTICLE INFO

Article history:
Received 22 January 2016
Received in revised form
25 May 2016
Accepted 2 June 2016
Available online 17 November 2016

Keywords:
Source apportionment
PMF
London
Hourly temporal resolution

ABSTRACT

London, like many major cities, has a noted air pollution problem, and a better understanding of the sources of airborne particles in the different size fractions will facilitate the implementation and effectiveness of control strategies to reduce air pollution. Thus, the trace elemental composition of the fine and coarse fraction were analysed at hourly time resolution at urban background (North Kensington, NK) and roadside (Marylebone Road, MR) sites within central London. Unlike previous work, the current study focuses on measurements during the summer providing a snapshot of contributing sources, utilising the high time resolution to improve source identification. Roadside enrichment was observed for a large number of elements associated with traffic emissions (Al, S, Ca, Ti, V, Cr, Mn, Fe, Ni, Cu, Zn, As, Rb and Zr), while those elements that are typically from more regional sources (e.g. Na, Cl, S and K) were not found to have an appreciable increment. Positive Matrix Factorization (PMF) was applied for the source apportionment of the particle mass at both sites with similar sources being identified, including sea salt, airborne soil, traffic emissions, secondary inorganic aerosols and a Zn-Pb source. In the fine fraction, traffic emissions was the largest contributing source at MR (31.9%), whereas it was incorporated within an "urban background" source at NK, which had contributions from wood smoke, vehicle emissions and secondary particles. Regional sources were the major contributors to the coarse fraction at both sites. Secondary inorganic aerosols (which contained influences from shipping emissions and coal combustion) source factors accounted for around 33% of the PM_{10} at NK and were found to have the highest contributions from regional sources, including from the European mainland. Exhaust and non-exhaust sources both contribute appreciably to PM_{10} levels at the MR site, highlighting the continuing importance of vehicle-related air pollutants at roadside.

1. Introduction

Exposure to airborne particles, both short and long-term, has been linked with a number of detrimental effects on human health (Cohen et al., 2005; Kampa and Castanas, 2008). The size and chemical composition of airborne particles are thought to be key factors affecting their toxicity (Heal et al., 2012). Smaller particles are thought by many to be more harmful than larger particles, and clear relationships have been observed between exposure to fine particles ($PM_{2.5}$, particles with an aerodynamic diameter less than 2.5 μm) and adverse health effects (Brook et al., 2010; Pope et al., 2002). As a result, $PM_{2.5}$ is an air pollution metric widely used to assess air quality, with the EU having set targets for reduction in $PM_{2.5}$ levels and population exposure.

In an urban environment, there are a number of sources, both natural and anthropogenic, which emit particles across a broad size

☆ This paper has been recommended for acceptance by Charles Wong.

* Corresponding author. Also at: Department of Environmental Sciences, Center of Excellence in Environmental Studies, King Abdulaziz University, PO Box 80203, Jeddah, 21589, Saudi Arabia.
E-mail address: r.m.harrison@bham.ac.uk (R.M. Harrison).

http://dx.doi.org/10.1016/j.envpol.2016.06.002

range. Sources typically differ for fine and coarse fractions, with fine particles most often from anthropogenic combustion sources, such as vehicle tailpipes, industrial emissions and biomass burning, and from secondary production within the atmosphere. In contrast, particles in the coarse fraction ($PM_{2.5-10}$, particles with an aerodynamic diameter between 2.5 and 10 μm) mainly arise from abrasion processes and can include crustal material and vehicle wear products (Minguillón et al., 2012; Richard et al., 2011). While trace metals typically only constitute a small proportion of the total particle mass (as low as 1% (Handler et al., 2008)), analysis of the elemental composition of ambient fine and coarse particle fractions can be effective in determining source contributions, particularly for measurements performed at a high time resolution (Gao et al., 2016; Visser et al., 2015a; Dall'Osto et al., 2013; Moreno et al., 2011; Viana et al., 2008).

London, like many major cities, has a noted air pollution problem, and a better understanding of the sources of airborne particles in the different size fractions will facilitate the implementation and effectiveness of control strategies to reduce air pollution. As a result there has been a concerted recent effort to characterise the sources of airborne particles in London, notably as part of the REgents PARk and Tower Environmental Experiment (REPARTEE) and Clean Air for London (ClearfLo) projects (Harrison et al., 2012a; Bohnenstengel et al., 2015). The ClearfLo project, included both long-term studies (e.g. Young et al., 2015a) as well as summer and winter intensive observational periods. There have been a number of source apportionment studies that have focused on the winter measurements investigating organic aerosols (Yin et al., 2015; Young et al., 2015b) and trace elemental datasets (Visser et al., 2015a). From these source apportionment studies it was found that during winter, major sources of primary organic aerosols were vehicle emissions and cooking (Yin et al., 2015). In addition, coarse fraction particles ($PM_{2.5-10}$) were influenced primarily by marine factors and traffic emissions whereas particles in the fine fraction (PM_1) were predominantly from more regional sources in winter (S-rich and solid fuel burning, Visser et al., 2015a).

A previous source apportionment analysis of a long-term (2 year) dataset comprising mainly trace element concentrations at an urban background site in London determined six sources; Urban background, Marine, Secondary, Non-exhaust traffic/Crustal, Fuel oil and Traffic (Beddows et al., 2015). This analysis was unable to fully resolve the traffic contributions, with the urban background source factor found to have a strong traffic signature, possibly due to the low time resolution (daily) of the measured elemental concentrations. Therefore in the present work we analyse trace elemental composition of particles in the fine and coarse fractions at an urban background and roadside site in London collected at a high (hourly) temporal resolution, with the aim to improve the source apportionment, particularly of traffic emissions. In contrast to previous studies in London using elemental analysis (Beddows et al., 2015; Visser et al., 2015a, 2015b), the current work focusses on measurements during the summer, and thus provides a snapshot of the contributing sources for this period. The results are compared at both roadside and urban background sites, in order to examine the contribution of vehicle emissions and its source characteristics. We employ a receptor model, Positive Matrix Factorization (PMF), to apportion the sources at both sites, utilising the high time resolution of the elemental data to improve the source identification. The resultant sources and size fractions determined for each site are compared to examine the differences in contributing sources.

2. Method

2.1. Sampling sites

The measurements were a part of the ClearfLo project (Clean Air for London, www.clearflo.ac.uk), which aimed to investigate boundary layer pollution in London; an overview is provided by Bohnenstengel et al. (2015). Sampling was conducted during the summer intensive observation period in July–August 2012 at two sites located within central London. The first site, classified as urban background, was within a school grounds in a residential area of North Kensington (NK). The air pollution climate at NK has been described in detail by Bigi and Harrison (2010), and is considered as representative of the background air quality for most of London. The second site, classified as roadside, was located 1 m from Marylebone Road (MR), a busy six lane road (ca. 80,000 vehicles a day) in central London. Both sites are also permanent stations of the Automatic Urban and Rural Network (AURN) from which monitoring data for the classical air pollutants were obtained. At both sampling sites black carbon (BC, 2 wavelength Aethalometer), nitrate (URG-9000B ambient ion monitor), NO_x (chemiluminescence) and $PM_{2.5}$ mass concentrations (FDMS-TEOM) were obtained from the national AURN and Speciation Networks. PM_{10} mass concentrations were available from the AURN for NK but not at MR due to instrument malfunction. A map detailing the locations of the sampling sites can be found in Bohnenstengel et al. (2015).

2.2. Sampling methodology and instrumentation

Aerosol samples were collected by low volume continuous 'Streaker' samplers, which allowed the determination of the elemental concentrations with hourly resolution, in both the fine (D_a < 2.5 μm) and the coarse (2.5 μm < D_a < 10 μm) fraction of particulate matter (Crespo et al., 2012; D'Alessandro et al., 2003). Briefly, in a Streaker sampler, particles are separated in two different stages by a pre-impactor and an impactor. The pre-impactor removes particulate matter with aerodynamic diameter D_{ae} > 10 μm. The aerosol coarse fraction impacts on a Kapton foil where it is deposited while the fine fraction is collected on a Nuclepore filter having 0.4 μm pores. The two collecting plates (Kapton and Nuclepore) are paired on a cartridge, which rotates at constant speed (~1.8° per hour) for a week: this produces a circular continuous deposit of particular matter (the 'streak') on both stages.

The resulting samples were analysed via PIXE (Particle-Induced X-Ray Emission) performed with 2.7 MeV protons from the 3 MV Tandetron accelerator of the **L**aboratorio di tecniche nucleari per l'**A**mbiente e i **BE**ni **C**ulturali (LABEC) laboratory of Istituto Nazionale di Fisica Nucleare (INFN) in Florence, with the external beam set-up described extensively elsewhere (Lucarelli et al., 2014). The beam (30–200 nA) scanned the streak in steps corresponding to 1 h of aerosol sampling; each spot was irradiated for about 180 s. The resulting PIXE spectra were fitted using the GUPIX software package (Maxwell et al., 1995) and elemental concentrations were obtained via a calibration curve from a set of thin standards of known areal density. The uncertainty of hourly elemental concentrations was determined by a combination of independent uncertainties in: standard sample thickness (5%), sampling parameters (5%) and X-ray counting statistics (2–20%). Detection limits were about 10 ng m^{-3} for low-atomic number elements and 1 ng m^{-3} or below for medium-high atomic number elements. The following elements were detected: Na, Mg, Al, P, S, Cl, K, Ca, Ti, V, Cr, Mn, Fe, Ni, Cu, Zn, Sr and Pb. Occasionally Bi was also detected. Unfortunately, the Nuclepore filters were contaminated by Si and Br whose ambient concentrations were consequently not possible to determine. We

analysed the filters collected between 20th July 2012 and 3rd August 2012 for a total sampling time of 306 h. Data coverage during this period was 91% at the NK and 98% at the MR site. The overlap between the two sites was high, with 90% of the time having simultaneous measurements.

At both sampling sites black carbon (BC), nitrate, NO_x, and $PM_{2.5}$ mass concentrations were obtained from the national AURN and Speciation Networks. PM_{10} mass concentrations were available from the AURN for NK but not at MR due to instrument malfunction.

2.3. Data analysis

Wind rose plots, diurnal variations and conditional probability function (CPF) analyses were all performed in R using the Openair package (Carslaw and Ropkins, 2012). CPF is a data analysis tool to find the direction of source contributions and was applied to both the elemental concentration and the PMF source factors. Polar plots are used to present the CPF analyses, where the number of events with a concentration greater than the 90th percentile is plotted as function of both wind speed and direction, as shown in Equation (1)

$$CPF = m_{\theta,j}/n_{\theta,j} \quad (1)$$

where $m_{\theta,j}$ is the number of samples in wind sector θ and wind speed sector j with a concentration greater than the 90th percentile and $n_{\theta,j}$ is the total number of samples with the same wind direction and speed (Carslaw, 2013). The resultant CPF polar plots present the probability that high concentrations of a pollutant came from a particular wind direction and speed (Carslaw, 2013) and can give insight into the contributions from local and regional sources. Wind data were derived from the Heathrow Airport site, which has previously proved to be a good indicator of air mass movements across London (Beddows et al., 2015).

2.3.1. PMF analysis

Positive Matrix Factorization (PMF) was applied to the hourly data sets from NK and MR, aiming at the identification and quantification of the major aerosol sources, using the EPA PMF5.0 software. PMF is an advanced factor analysis technique based on a weighted least square fit approach (Paatero and Tapper, 1994); it uses realistic error estimates to weight data values and imposes non-negativity constraints in the factor computational process. Briefly, the PMF factor model can be written as $X = G \cdot F + E$, where X is a known n by m matrix of the m measured chemical species in n samples; G is an n by p matrix of source contributions to the samples (i.e. time variations of the p factor scores); F is a p by m matrix of factors composition (often called source profiles). G and F are factor matrices to be determined and E is defined as a residual matrix. In addition to the elemental data, concentrations of BC (fine fraction only) and nitrate (measured in PM_{10} and included in both fine and coarse fractions) were included in the analysis. Input data were prepared using the procedure suggested by Polissar et al. (1998). Since PMF is a weighted least-squares method, individual estimates of the uncertainty in each data value are needed. The uncertainty estimates were based on the approaches by Polissar et al. (1998). Species that retained a significant signal were separated from the ones dominated by noise, following the signal-to-noise (S/N) criterion defined by Paatero and Hopke (2003). Species with $S/N < 0.2$ are considered as bad variables and removed from the analysis and species with $0.2 < S/N < 2$ are defined as weak variables and down weighted by a factor of 3. Nevertheless, since S/N is very sensitive to sporadic values much higher than the level of noise, the percentage of data above detection limit was used as a complementary criterion. PMF results for a different number of factors and multiple values of FPEAK were systematically explored to determine the most reasonable solution (20 pseudorandom initializations were run for each test). As PMF is a descriptive model, there are no objective criteria for choosing the right number of factors (Paatero et al., 2002). Therefore a number of criteria were applied including extracting realistic source profiles, distribution of scaled residuals, Q/Q_{exp} and the comparison between the PMF modelled and measured elemental mass. For selecting a PMF solution, the key criterion applied was based on extracting realistic and reasonable source profiles and contributions. This included the extracted sources demonstrating diurnal profiles as expected for that source and logical correlations with external tracers (e.g. NO_x with traffic sources). The Q/Q_{exp} index was monitored with increasing number of factors, as a large decrease is indicative of increased explanatory power in the model of the data, while a small decrease suggestive of little improvement with extra factors. Consequently, the number of factors was chosen after Q/Q_{exp} decreased significantly. The G and F factor outputs were normalised against the particle mass concentrations. At MR, there was no PM_{10} mass concentration data available from the AURN and so the G and F factor outputs were normalised against a reconstructed mass. The reconstructed mass for the coarse fraction at MR was calculated by summing the estimated concentration of sulphate and nitrate salts, crustal metal oxides and sea spray from measured elemental concentrations based on molecular weight ratios. The FPEAK parameter explores the rotational ambiguity of the solution (see Paatero (2000) for more details), and as changing the FPEAK value did not appear to improve the source profiles, base model results are shown (FPEAK = 0).

3. Results and discussion

3.1. Average concentration at MR and NK sites

The average concentrations of the analysed elements for each site and size fraction is shown in Fig. S1, with summary statistics for both sites and size fractions provided in Tables S1–4 (Supporting Information). From Fig. S1, the most abundant elements were (in order) Fe, S, Cl, Ca, Si and Na, which are typically primarily of crustal or marine origin, while the elements with a greater anthropogenic contribution such as Cu, Zn and Pb had lower concentrations. Generally, MR had higher concentrations than NK. In the fine fraction, all elements except for Na, P, Se and Pb had statistically significantly higher ($p < 0.05$) concentrations at MR compared to NK. In the coarse fraction, Na, Mg, Si, P, Cl, K, Se, and Br were present at similar concentrations at both sites, while all other elements had statistically significantly higher concentrations ($p < 0.05$) at MR compared to NK. Thus in both fractions the majority of elements (Al, S, Ca, Ti, V, Cr, Mn, Fe, Ni, Cu, Zn, As, Rb, Zr) exhibited roadside enrichment, as did Mo and Pb in the coarse fraction, and likely had a contribution from sources related to traffic emissions. The elements that recorded similar concentrations at both sites are indicative of sources unrelated to vehicle emissions and include sea salt (Na, Cl, Mg), biomass burning (K) (Chow et al., 2007; Harrison et al., 2012b) and industrial emissions (e.g. Pb and Sr) (Dall'Osto et al., 2013; Widory et al., 2010). The observed roadside enrichment levels in this study are broadly consistent with previous work at these sites (Visser et al., 2015b).

As expected, BC shows a huge enrichment at MR as a result of its presence in diesel engine emissions (Tables S1 and S3). Less expected is the enrichment of nitrate, with almost double the mean concentrations observed at MR compared to NK (Tables S2 and S4). This could result from enhanced NO_x oxidation in the street canyon, which seems unlikely given the short residence times of the air. It might also be due to emissions of ammonia from vehicles causing

Table 1
Summary of the PMF solutions at NK and MR. The contribution refers to the percentage of the total particle mass, with the average particle mass given (μg m^{-3}), with the exception of the coarse fraction at MR which was normalised to a reconstructed particle mass. Hence concentrations reported for MR coarse fraction refer to the percentage of detected particle mass (μg m^{-3}). SIA refers to secondary inorganic aerosols.

Site	NK		MR		NK		MR	
Fraction	Fine		Fine		Coarse		Coarse	
	Source	Contribution	Source	Contribution	Source	Contribution	Source	Contribution
1	Sea Salt	5.1%	Sea Salt	9.8%	Fresh sea salt	22.2%	Fresh sea salt	7.0%
2	SIA	31.4%	SIA (1)	21.8%	Aged sea salt	12.9%	Aged sea salt/nitrate	42.3%
3	Soil	10.4%	Construction	8.6%	Soil	16.2%	Construction	6.3%
4	Traffic	10.2%	Traffic	32.6%	Traffic	17.8%	Vehicle wear	13.4%
5	Zn-Pb	4.0%	Zn-Pb	0.5%	Nitrate	31.0%	Re-suspended road dust	31.0%
6	Urban background	39.0%	SIA (2)	26.8%	–	–	–	–
Particle Mass	**11**		**21**		**6**		**10**	

enhanced conversion of nitric acid vapour to particulate nitrate. However, concentrations of ammonium were similar at the two sites (0.98 ± 0.7 μg m^{-3} at NK and 0.94 ± 0.9 μg m^{-3} at MR), so this is thought unlikely.

The size distribution of individual elements was similar across both sites, with S, Ni, Zn, As, Se and Pb having higher concentrations in the fine fraction, while Na, Mg, Al, P, Cl, Ti, Mn, Fe, Cu, Rb, Zr and Mo had higher concentrations in the coarse fraction ($p < 0.05$). At MR Ca, Cr and Sr had a similar concentration across both size fractions whereas at NK, Ca and Sr were found preferentially in the coarse fraction and Cr in the fine fraction. Typically elements from combustion sources are found preferentially in the finer particles (Minguillón et al., 2012), and thus fossil fuel combustion and industrial emissions may be a source of S, V, Ni, Zn, As, Se and Pb (Dall'Osto et al., 2013; Moreno et al., 2010; Ning et al., 2008). Mechanically generated sea salt particles are normally found in the coarser size fraction which further points to a marine source for Na, Mg and Cl. As expected, elements normally associated with a crustal source, such as Al, Ca, Ti, Fe were generally found preferentially in the coarse fraction (Minguillón et al., 2012; Richard et al., 2011), with the exception of Ca at MR, which suggests an additional source. Soil Enrichment Factors (EF) were calculated for these crustal elements, using Al as reference element and the crustal composition given by Taylor (1964), see Table S5, Supporting Information. The calculated EF was generally close to 1 for Si and K, Ca, Ti and Sr in the coarse fraction, indicating that crustal material was the main source. The exception was during episodic peaks in concentration of K, Ca and Sr (See Fig. S2), when the EF was greater than 1, indicating that were other sources of these elements. Fe had a higher EF than the other crustal elements, as there are other sources of Fe such as vehicle abrasion processes. Particles emitted by these abrasion processes, such as brake and engine wear, have been shown to be in both the coarse and fine fractions and in addition to Fe include elements such as Mn, Cu, Rb, Zr and Mo (Richard et al., 2011; Thorpe and Harrison, 2008), supporting this source assignment for these elements, particularly with the observed roadside enrichment.

3.2. Source apportionment by PMF

PMF analysis was performed separately at NK and MR for the fine and coarse datasets independently. In all of the presented PMF solutions, most of the scaled residuals (portion of data for each element unexplained by model divided its uncertainty) were between ±3.0 and normally distributed, as suggested by Paatero and Hopke (2003). Furthermore, concentrations of all species were reconstructed to within 20% by the model with a few exceptions. As there is no organic component included in the PMF, the presented particle mass contributions are representative of the measured species, and hence the majority of the particle mass. The resultant solutions at NK and MR are summarised in Table 1, with 6 and 5 factor solutions chosen for the fine and coarse fraction, respectively at both NK and MR. The source profiles are given in Figs. 1–4 while the times series can be found in the Figs. S3–7, Supporting Information. Overall, similar sources were observed at MR and NK, with the exception of a construction dust source identified only at MR and a nitrate and urban background source at NK (Table 1). As expected, as MR is a roadside site, higher traffic contributions were observed at MR compared to NK (Table 1). A detailed description of the identified sources at NK and MR is presented in the following sections.

3.2.1. Sea salt/marine sources

At both sites, there were factors that were characterised by notable contributions from the typical marine elements Na, Mg and Cl, which was the basis for assigning these factors to sea salt particles.

At both sites, only one sea salt source was identified in the fine fraction, while there were two coarse fraction marine sources identified. While Na and Mg had notable contributions in both coarse marine sources, the two sources were differentiated based on the level of Cl (Figs. 2 and 4) and were assigned to aged and fresh sea salt particles. For both the aged and fresh sea salt sources, the Na/Mg ratio was comparable to the expected ratio for seawater (4–6), along with the Na/Cl ratio in the fresh sea salt factors (0.6). In the aged sea salt factors, Cl levels were almost zero presumably resulting from the well-known heterogeneous reactions between airborne sea-salt particles and acidic pollutants (e.g. nitric and sulfuric acid), which result in the volatilization of HCl (Seinfeld and Pandis, 1998; Singh, 1995). In the fine fraction, the single marine source at NK and MR showed Cl/Na ratios well below those of seawater indicating substantial ageing but still had a substantial contribution from Cl unlike coarse aged sea salt (Figs. 1–4). At both sites, the fine fraction marine source was well correlated (r^2 of 0.85) with the fresh sea salt factors unlike the aged sea salt ($r^2 < 0.2$) in the coarse fraction, suggesting that the fine marine source was indeed sea salt.

At both MR and NK, application of CPF analysis found that the highest source contributions for the two coarse fraction marine sources came from different directions, with the results shown in Fig. 5. For the fresh sea salt particles, highest contributions were from the south/southwest at high wind speeds (Fig. 5), with similar results observed for the fine fraction sea salt factors (Fig. S7, Supporting Information). During sampling, the prevailing wind direction was from the south/southwest (Fig. S8, Supporting Information) and is the likely reason why the highest contributions for fresh sea salt were from the south/southwest, even though the closest coastline to London is to the east. The highest contributions

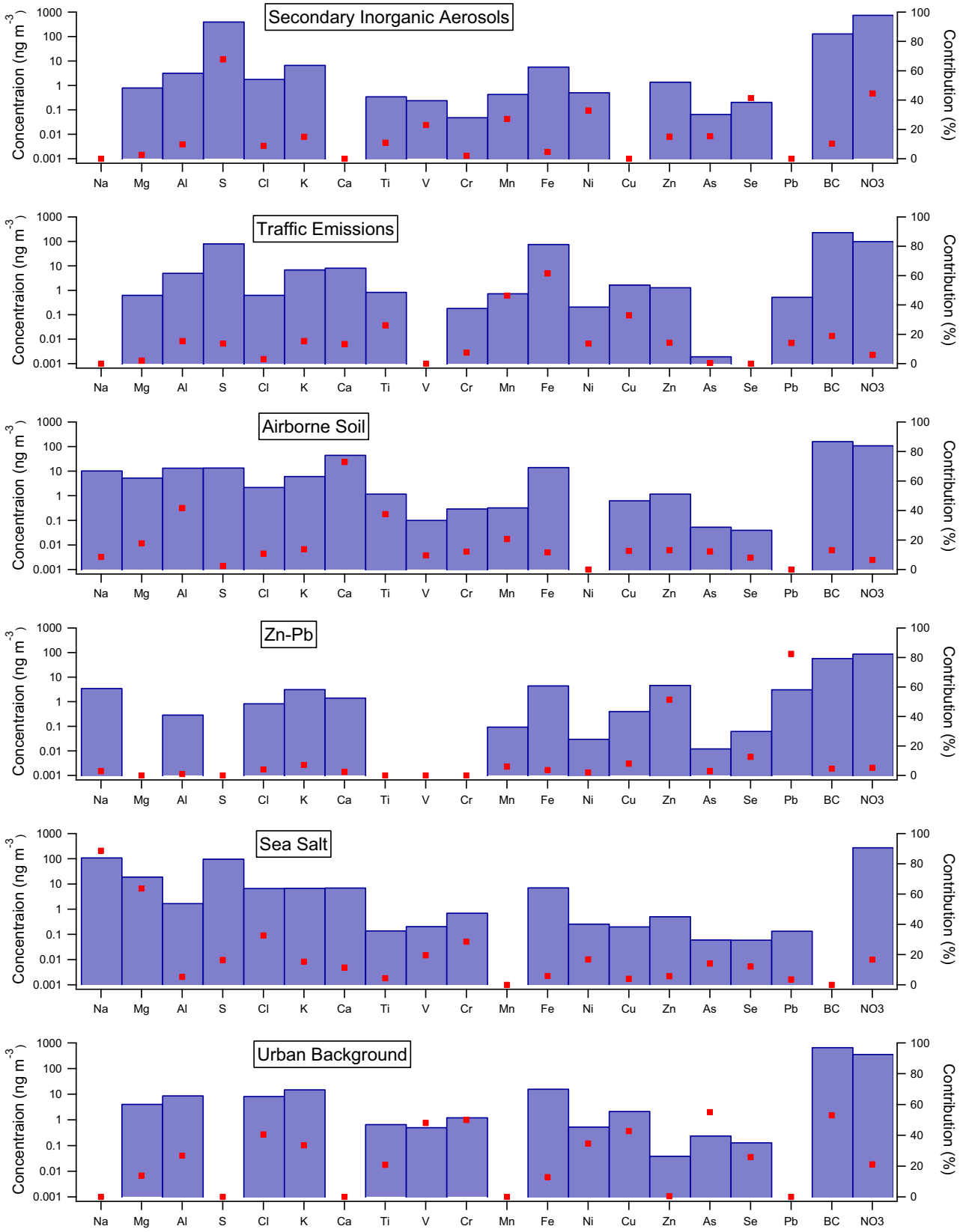

Fig. 1. Source profiles for the six factor solution at NK in the fine fraction. Blue bars represent concentration (ng m^{-3}) while the red squares indicate the percentage contribution to total mass for each constituent. (For interpretation of the references to colour in this figure legend, the reader is referred to the web version of this article.)

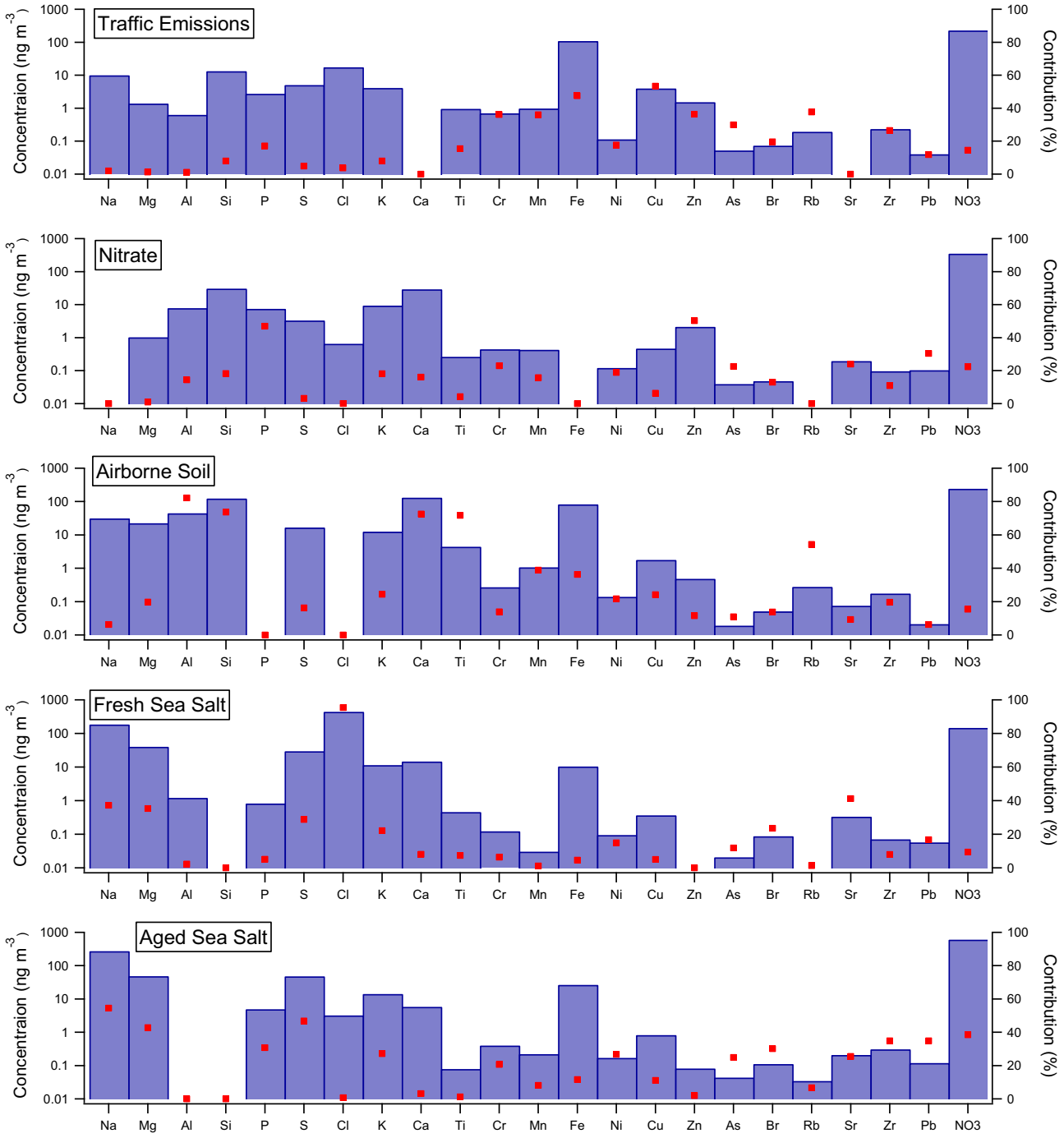

Fig. 2. Source profiles for the five factor solution at NK in the coarse fraction. Blue bars represent concentration (ng m^{-3}) while the red squares indicate the percentage contribution to total mass for each constituent. (For interpretation of the references to colour in this figure legend, the reader is referred to the web version of this article.)

for the aged sea salt factors were from the east/north east at lower wind speeds (Fig. 5), possibly as a result of the interaction of sea salt from the North Sea with polluted air masses from the European mainland, further supported by the notable contributions from elements not normally associated with marine sources (e.g. Cr, Sr, Mo, Pb; see Figs. 2 and 4). The coarse aged sea salt at MR (Fig. 4) shows a very high concentration of nitrate and this factor has hence been called aged sea salt/nitrate. Chloride ion volatilization as well as nitrate and sulphate formation is due to different reactions between airborne sea-salt particles and pollutants such as nitric and sulfuric acid (Seinfeld and Pandis, 1998; Singh, 1995). Thus, this source is a mixture of anthropogenic and natural contributions. It also shows some temporal features (Fig. S6), which are very similar to those of the NK coarse nitrate factor (Fig. S4).

3.2.2. *Airborne soil and construction dust*

PMF factors were identified at each site, which were characterised by contributions from the typically crustal elements Al, Si, Ca and Ti, and to a lesser extent Mg, K, Mn, Fe and Sr (see Figs. 1–4). The factor elemental profiles in the coarse fraction are shown in

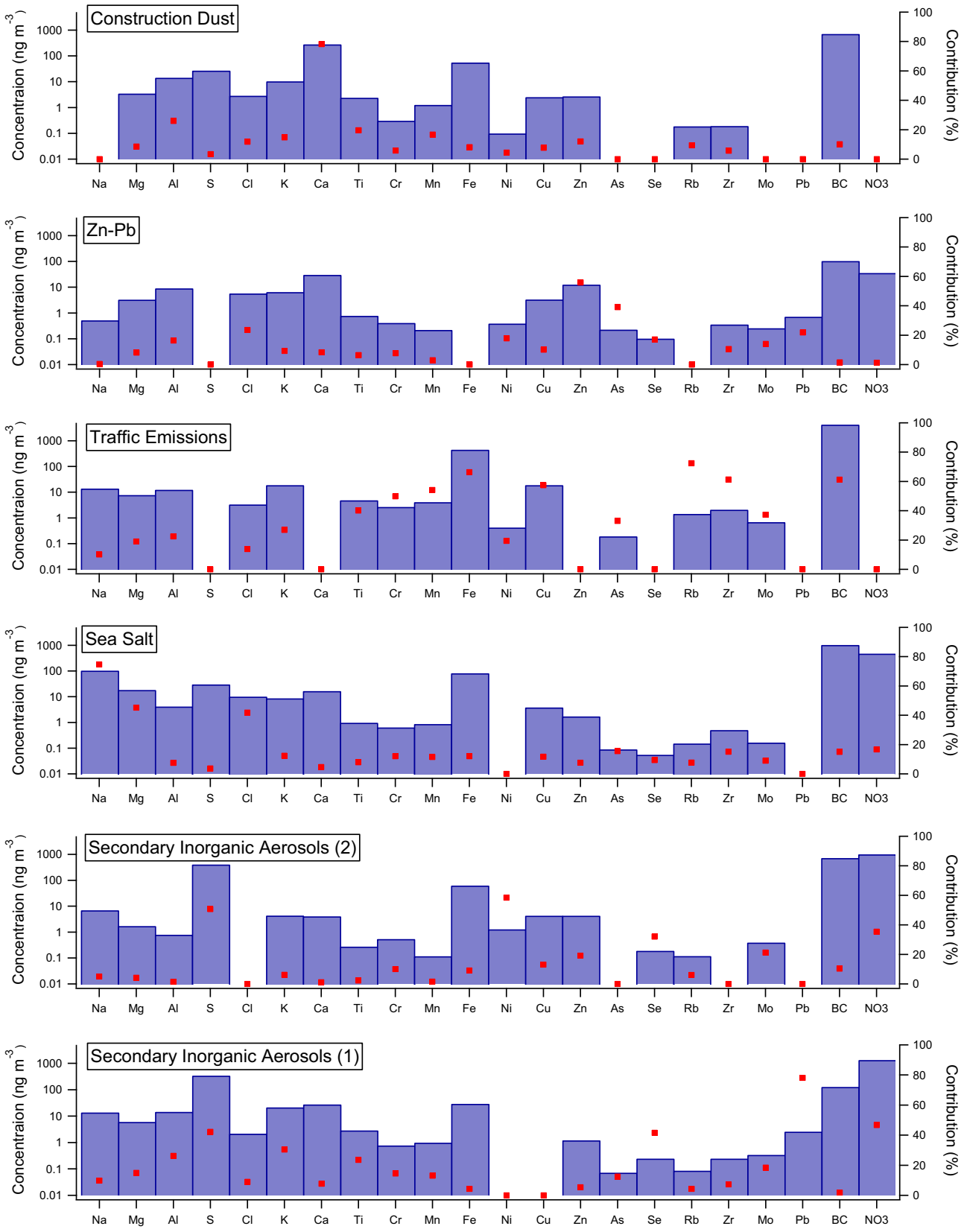

Fig. 3. Source profiles for the six factor solution at MR in the fine fraction. Blue bars represent concentration (ng m^{-3}) while the red squares indicate the percentage contribution to total mass for each constituent. (For interpretation of the references to colour in this figure legend, the reader is referred to the web version of this article.)

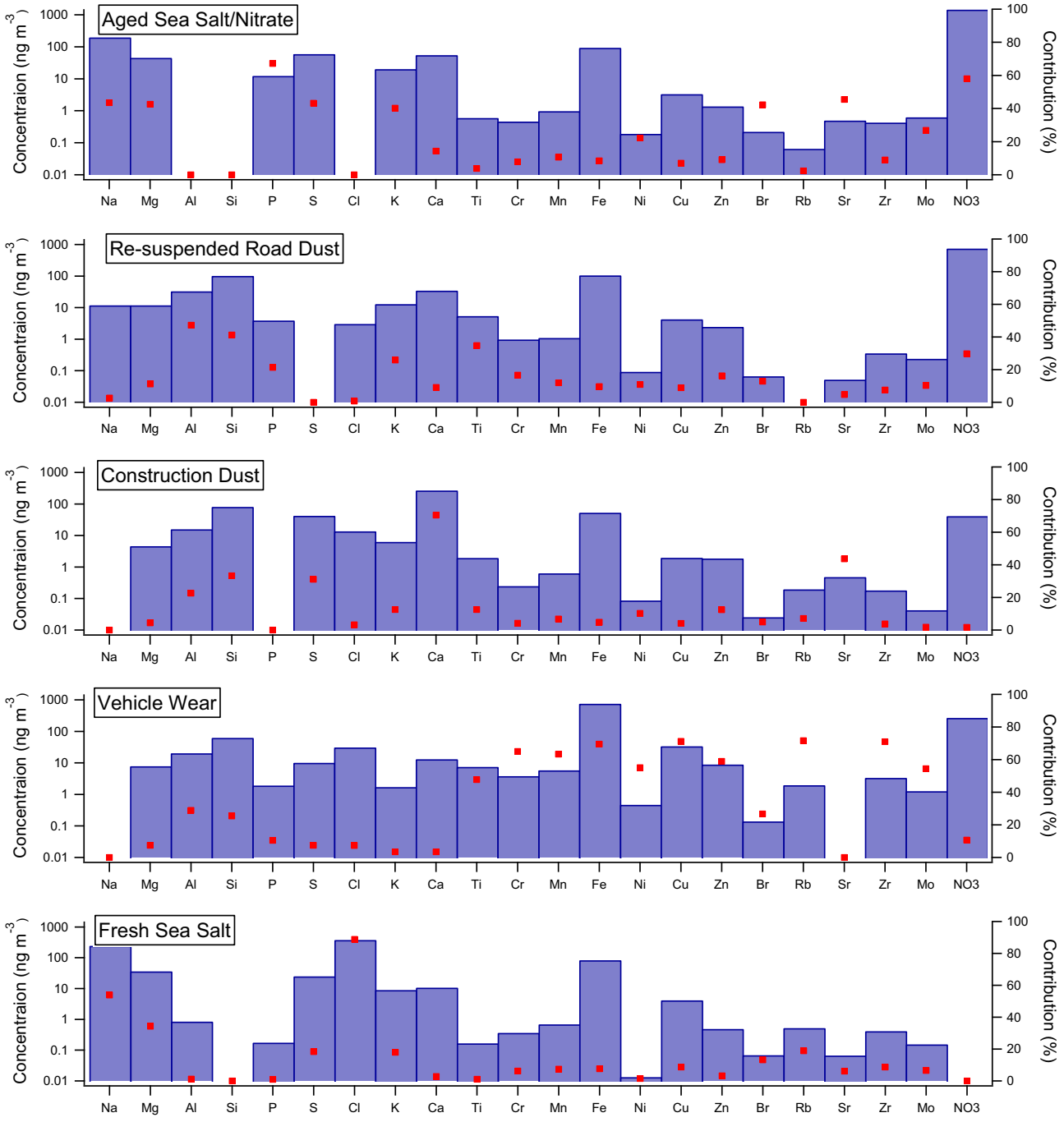

Fig. 4. Source profiles for the five factor solution at MR in the coarse fraction. Blue bars represent concentration (ng m^{-3}) while the red squares indicate the percentage contribution to total mass for each constituent. Note the presented source concentrations were normalised to a reconstructed particle mass, hence are representative of the detected particle mass. (For interpretation of the references to colour in this figure legend, the reader is referred to the web version of this article.)

Fig. 6 for both sites, normalised to Al along with a comparison to the average upper continental crust (UCC) values (Taylor, 1964). From Fig. 6, based on distinct differences observed in the elemental profiles and diurnal cycles, these factors were assigned to different sources; airborne soil particles, construction dust, and re-suspended road dust.

Present in both size fractions at MR was a source characterised by high loadings from Ca (EF of around 37) and Sr (EF of 7) compared to the soil source (Fig. 6), two elements that have previously been associated with construction and cement work (Bernardoni et al., 2011; Dall'Osto et al., 2013; Widory et al., 2010), and was therefore assigned to construction dust. Further evidence is found in the diurnal concentration profile, which peaked during the day and decreased to almost zero outside of normal working times (8am until 4pm), shown in Fig. 7 for the coarse fraction. A similar diurnal cycle was observed in the fine fraction (Supporting Information, Fig. S9). The temporal pattern of the construction factor is in agreement with results reported in Dall'Osto et al. (2013) and Vecchi et al. (2009) who also found a high correlation between Ca and S hourly concentrations during construction works, thus

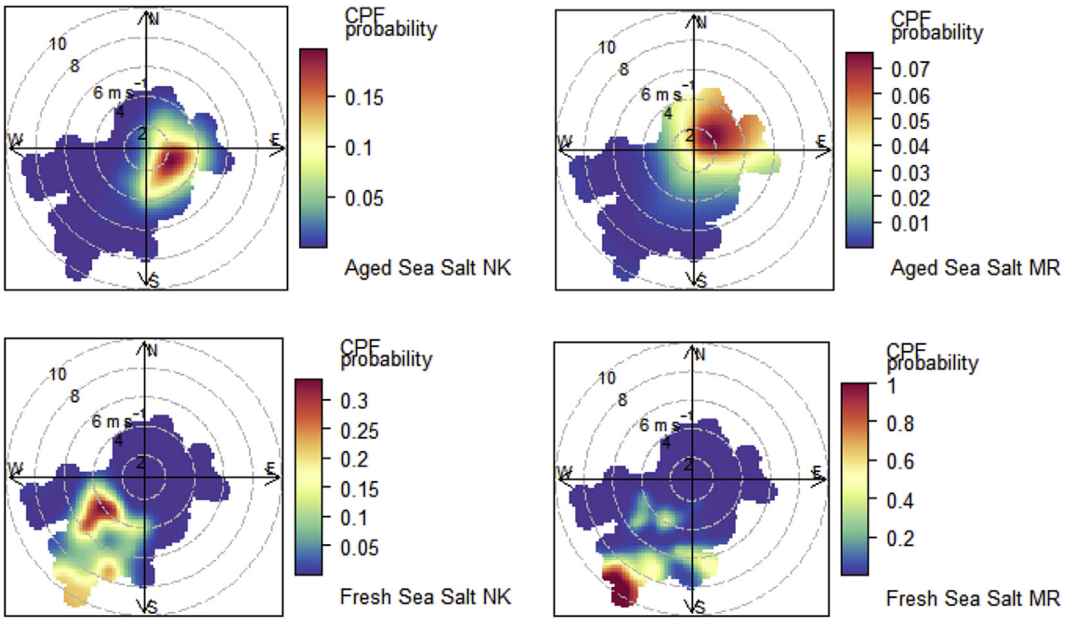

Fig. 5. CPF analysis of the aged and fresh sea salt factors in the coarse fraction at NK (left column) and MR (right column). Wind speed is in m s^{-1}.

supporting the high normalised concentrations for S and Ca reported in Fig. 6.

At MR in the coarse fraction, the source profile and diurnal cycle of the second crustal source had characteristic differences compared to the construction dust source. Along with Al, Si, Ca and Ti, elements associated with traffic emissions (Mn, Ni, Zn and Br, see Section 3.2.3) had notable contributions in this factor (Fig. 4). While the observed cycle was not as expected for traffic emissions (Fig. 7), the observed concentration peak that coincided with morning peak hour traffic, points to traffic as a contributing source. Thus, along with the contributions from traffic related elements, this factor was assigned to re-suspended road dust.

The soil source factor observed at NK in both fractions had a similar profile to the UCC, with the elements Mg, Si, K and Ti observed to have a EF (calculated with respect to Al) of around 1. Of the other crustal elements, in both size fractions Ca had a high EF (~6), which points to a notable influence from construction work. Mn and Fe also had a high enrichment (EF between 2 and 3), suggestive of traffic emissions as the source of the additional Fe. Furthermore in both size fractions, the diurnal cycle of the soil factor peaked at around 7–8am (Fig. S10, Supporting Information), similar to the re-suspended road dust factor at MR (Fig. 7), suggesting an influence from this source. Therefore, at NK this factor likely had a combined influence from airborne soil and construction dust.

3.2.3. *Traffic emissions*

A factor was attributed to traffic emissions for both size fractions at MR and NK, based primarily on the chemical profiles (Figs. 1–4) and the diurnal cycles (Fig. 8). At MR the traffic-related source factors differed between the two size fractions and were distinguished primarily by their source profiles. In the fine fraction at MR, the traffic factor accounted for the majority of the BC (Fig. 3), a typical marker for vehicle exhaust emissions but also included notable contributions from elements that are normally associated more with vehicle wear particles e.g. Cr, Mn, Cu, Fe, Zr and Mo (Thorpe and Harrison, 2008). In the coarse fraction at MR, the traffic factor had high contributions from Ti, Cr, Mn, Fe, Ni, Cu, Rb, Zr and Mo (Fig. 4), elements that have been previously associated with tyre, engine and brake wear particles (Pant and Harrison, 2013 and references therein). Both traffic factors at MR exhibited a more strongly bi-modal cycle that followed times of peak traffic (Fig. 8)

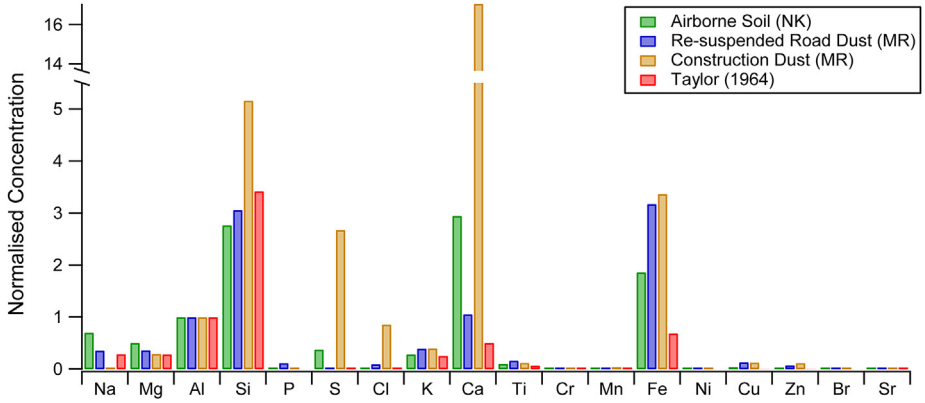

Fig. 6. Normalised concentrations of the soil and construction dust source profiles in the coarse fraction at MR and NK. The average continental upper crust composition is also reported for comparison (Taylor, 1964) and all values are normalised to the concentration of Al.

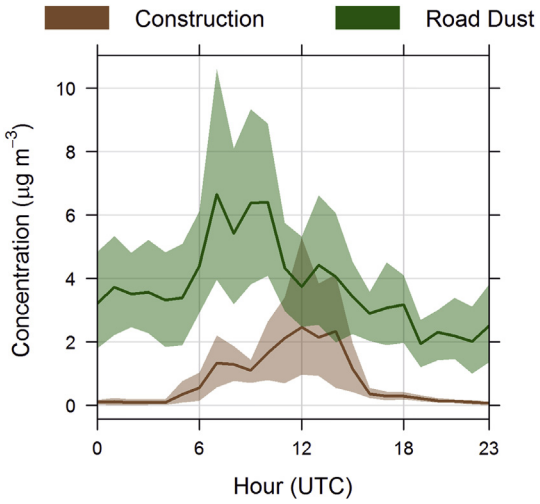

Fig. 7. Diurnal cycles of the re-suspended road dust and the construction dust factors at MR in the coarse fraction. Shaded areas represent the 95% confidence intervals. Note the presented source concentrations were normalised to a reconstructed particle mass, hence representative of the detected particle mass.

unlike that observed for NOx (Fig. S11, Supporting Information), likely due to the high braking load for vehicles in peak traffic, resulting in increased emissions of vehicle wear particles. Thus it would suggest that in the coarse fraction the main source was vehicle wear emissions, as particles emitted by this source are typically found more in the coarse fraction (Pant and Harrison, 2013 and references therein). However in the fine fraction, the observed high loadings from BC point to a strong influence from exhaust emissions, hence our assignment to more general traffic emissions.

As seen in Fig. 8, at NK there was a factor in each size fraction with a bi-modal diurnal cycle comparable to the diurnal trends for NO_x (Fig. S11), which was correlated with NO_x concentrations (r^2 of 0.51), implicating traffic emissions as the source. In both fractions at NK, the traffic factor profiles had high loadings from Cr, Mn, Fe, Cu, which are typical brake and engine wear elements and points to vehicle wear emissions as a contributing source.

Furthermore, the fine fraction traffic emission factor at NK did not account for the majority of BC; rather it was another factor which also had high loadings from Cl, K, V, Cr, Cu and As (Fig. 1). This elemental profile does not clearly indicate a source but a number of these species (e.g. V, Cr, Cu, As and BC) have been previously associated with vehicle exhaust emissions (Ning et al., 2008; Pant et al., 2014). Furthermore, the diurnal profile (Fig. S12, Supporting Information) was similar to that observed for NOx (Fig. S11), suggesting vehicle emissions as a source. However, the high loading from K and BC can also point to an influence from wood smoke (Crilley et al., 2015) in addition to vehicle emissions. Beddows et al. (2015) previously identified at NK in a year-long dataset a factor, which had no clear source but had contributions from both wood smoke and traffic emissions and named it an "urban background" source. Therefore, this factor was also assigned to an urban background source. The large nitrate concentration (Fig. 1) and large nocturnal concentrations suggests a secondary

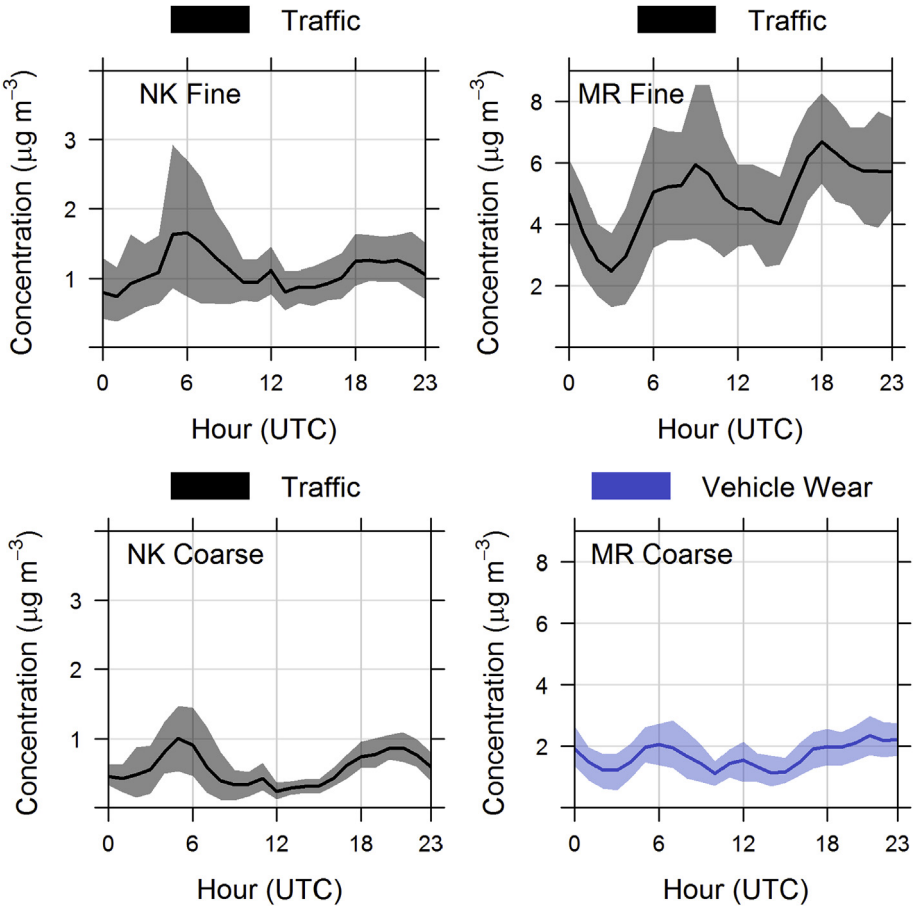

Fig. 8. Diurnal cycles of the traffic related factors in the fine fraction (top row) and coarse fraction (bottom row) at NK (left) and MR (right). Shaded areas represent the 95% confidence intervals. Note the different y-axis scales for NK compared to MR. Note the presented source concentrations at MR coarse fraction were normalised to a reconstructed particle mass, hence representative of the detected particle mass, unlike the other three analyses (MR fine, NK fine and coarse).

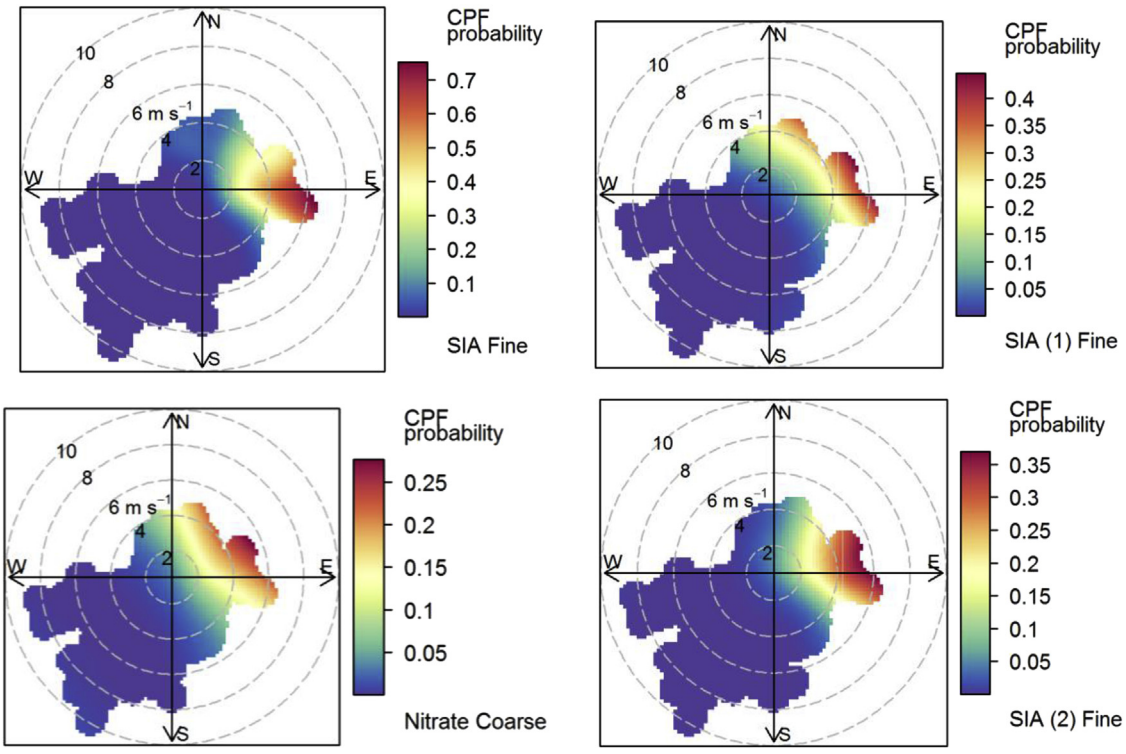

Fig. 9. CPF analysis polar plots of the secondary inorganic aerosols factors at NK (left column) and MR (right column). The size fraction for each factor is also indicated. Wind speed is in m s^{-1}.

contribution to this factor.

As the PMF analysis for the coarse fraction at MR was normalised to a reconstructed particle mass, direct comparison between the absolute concentrations to other PMF analyses, which were normalised to measured total particle mass, are not valid. Therefore, considering the fine fraction only, higher contributions from the traffic emission factors were observed at the roadside site (MR) compared to the urban background site (NK), as expected (Table 1 and Fig. 8). Furthermore, using reconstructed particle mass may explain why traffic emissions appear to have much higher contributions in the fine compared to the coarse fraction at MR (Fig. 8). However, if the coarse re-suspended road dust factor (also attributed to traffic emissions, see previous section), is combined with the vehicle wear factor, traffic emissions contributed roughly equal proportion to fine and coarse fractions (Table 1), in agreement with previous results (Harrison et al., 2001; Querol et al., 2004).

3.2.4. Secondary inorganic aerosol

At both sites in the fine fraction, there were factors characterised by high loadings from S, Se and nitrate, which were assigned to secondary inorganic aerosol (SIA, Figs. 1 and 3). Two such SIA sources were identified at MR, with one accounting for a large percentage of Ni (SIA (2)) and the other characterised by higher loadings of crustal elements and Pb (SIA (1)), suggesting different primary sources contributed to the SIA, such as fuel oil combustion for SIA (2). The time series for the SIA (1) and (2) factors at MR were not correlated (r^2 of 0.02), combined with the observed notable differences in source profile (Fig. 3) suggests that these are two distinct sources rather than 'splitting' of one factor. The differences in source profiles suggest different primary sources contributing to the formation of SIA. Only one SIA factor was identified at NK, possibly as the second was indistinguishable from the urban background source, which also had high contributions from Se and Ni (Fig. 1). The two MR SIA time series were correlated with the SIA at NK, with SIA (2) more correlated than SIA (1) (r^2 of 0.72 and 0.41, respectively). The high loadings from S, Ni and Se, established tracers for oil combustion and coal combustion (Moreno et al., 2010, 2013), point to shipping and power plant emissions as contributing sources. Both of these sources emit large quantities of SO_2, which reacts in the atmosphere to form sulphate and could explain the overlapping sources. CPF analysis (Fig. 9) indicated that the for all SIA factors the highest contributions were from the east at high wind speeds at both sites, suggesting similar source locations. In this easterly direction lie a number of industrial activities including power stations and major east coast ports of Felixstowe and Harwich, which may contribute.

In addition, a source was identified at NK in the coarse fraction characterised by high contributions to crustal elements (e.g. Al, Si, K and Ca), Zn, Pb and nitrate (Fig. 2). The coating of nitrate on the surfaces of mineral dust particles formed by heterogeneous reactions is well known (see e.g (Li and Shao, 2009; Usher et al., 2003). but the concentrations of elements such as Ca which is known to bind with nitrate appear insufficient, and hence its composition may be that of ammonium nitrate. Minguillón et al. (2012) also observed high loadings of Zn and Pb in an ammonium nitrate source in the coarse fraction. This nitrate factor was correlated with the SIA factors (r^2 of 0.4–0.5) and CPF analysis also indicated the highest contributions from regional sources to the east (Fig. 9). Furthermore, the CPF results for the SIA and nitrate (Fig. 9) are in agreement with Charron et al. (2013), who demonstrated that long-range transport of secondary particles (including sulphate and nitrate) originating from mainland Europe were a significant source of particles in London. Overall, secondary inorganic aerosols accounted for a considerable portion of the fine particle elemental mass at MR and the coarse and fine elemental mass at NK (Table 1). This result suggests that regional sources, which include emissions from industrial plants and shipping located to the east of London, have a significant influence on the fine particle composition in London, consistent with the conclusions of Beddows et al. (2015) based upon an analysis of 24 months

of data.

3.2.5. Zn-Pb factor

A factor was identified in the fine fraction at NK and MR accounting for a high proportion of the variance of Zn and Pb (Figs. 1 and 3), although the main chemical constituents were in both cases BC and nitrate. The time series for these factors was characterised by a number of episodic peaks, suggesting an industrial source (Figs. S3 and S5). Based on the high contributions from Zn and Pb, the source may be industrial emissions such as metal workshops or smelters (Dall'Osto et al., 2013; Moreno et al., 2013; Richard et al., 2011). However, at MR the diurnal cycle demonstrated a clear peak at around 9am (Fig. S13, Supporting Information), suggesting there may have been influence from a source related to traffic as well. Overall, this factor accounted for a small percentage (<4%) of the total fine fraction particle mass at MR and NK, and so does not represent a significant source.

3.3. Comparison to previous source apportionment in London

Previous source apportionment studies of airborne particles utilising elemental datasets in London were conducted in winter (Visser et al., 2015b) or on long-term datasets (Beddows et al., 2015). Thus, while quantitative comparison to current work is problematic owing to the different seasons covered, qualitative evaluation of the sources identified is possible. In addition, while Beddows et al. (2015) applied a similar source apportionment technique to the current work, albeit to 24 h samples, Visser et al. (2015a) utilised a different methodology. Nevertheless, while there were similar sources identified overall (e.g. marine, secondary, traffic and crustal), some notable differences were evident between the three studies. Beddows et al. (2015) identified an urban background factor, which had influences from wood smoke and traffic, and despite the higher time resolution a similar factor was also extracted for the fine fraction at NK in the current study. That this source was identified by both studies with datasets of differing time resolutions would appear to underline the difficulty in separating co-linear sources in the urban background.

The use of higher time resolution data did improve source identification, with a distinct solid fuel burning source identified during the winter (Visser et al., 2015a) probably due to (expected) seasonal variation in emissions due to heating. An industrial source, characterised by episodic concentration peaks, was found both in the present study and Visser et al. (2015a), possibly due to the higher time resolution of the elemental data in these studies compared to Beddows et al. (2015). However, the industrial sources were characterised by different elements; Cr and Ni (Visser et al., 2015a), and Zn and Pb (present work) suggesting different sources (or activity). It is noteworthy that the urban background factor described in Beddows et al. (2015) also contained high loadings from Zn and Pb. Separate traffic factors were extracted in all three studies (Beddows et a. 2015; Visser et al., 2015a; present work), there was however variation in the proportional contributions from traffic to the particle size fractions. For the long-term measurements of Beddows et al. (2015), only 4.5% of PM_{10} mass was accounted for at NK by a distinct traffic factor, much lower than that observed in the current work (Table 1). This may be due to higher time resolution in the current work enabling better discrimination of vehicle emissions from the urban background factor. Visser et al. (2015a) observed that traffic-related factors were mainly in the coarse mode, whereas in the current work the traffic sources were found to be more evenly distributed across the size fractions (Table 1). This difference may be due to the different species (e.g. BC) and source apportionment techniques between the current work and Visser et al. (2015a).

4. Conclusions

The trace elemental composition of the fine and coarse fractions of airborne particles were analysed during summer 2012 at a high time resolution at urban background and roadside sites within central London to examine the contributing sources. Roadside enrichment was observed for a large number of elements associated with traffic emissions (Al, S, Ca, Ti, V, Cr, Mn, Fe, Ni, Cu, Zn, As, Rb and Zr) while those elements that are typically from more regional sources (e.g. Na, Cl, S and K) were not found to have an appreciable increment. PMF was applied for the source apportionment of the particle mass at both sites with similar sources being identified, which included sea salt, airborne soil, traffic emissions, secondary inorganic aerosols and an industrial (Zn-Pb) source. In addition, a distinct construction dust source factor was identified at MR, though the airborne soil source factor at NK had evidence of possible influence from construction activities. Distinct sources were also identified at NK and include urban background and nitrate sources. Utilising high time resolution elemental data was found to improve the source apportionment compared to previous work in London (Beddows et al., 2015), notably for sources that have a distinct temporal variation in their emissions, such as traffic emissions and construction activities.

In the fine fraction, traffic emissions were the largest contributing source at MR whereas at NK it was an urban background source, with combined contributions from both wood smoke and vehicle emissions. In the coarse fraction the largest sources were regional sources (nitrate and aged sea salt). Secondary inorganic aerosol (which notably contained influences from shipping emissions and coal combustion) accounted for around 33% of the PM_{10} at NK and was found to have the highest contributions from regional sources, possibly from the European mainland. These results suggest that emissions from industrial plants and shipping located to the east of London have a significant influence on the PM_{10} particle composition in London. This is consistent with earlier work (Charron et al., 2007), which demonstrated the importance of both local and regional sources in contributing to exceedences of the daily limit value for PM_{10} of 50 $\mu g\ m^{-3}$.

Acknowledgements

The ClearfLo project was funded by the UK Natural Environment Research Council (NE/H003142/1).

Appendix A. Supplementary data

Supplementary data related to this article can be found at http://dx.doi.org/10.1016/j.envpol.2016.06.002.

References

Beddows, D.C.S., Harrison, R.M., Green, D.C., Fuller, G.W., 2015. Receptor modelling of both particle composition and size distribution from a background site in London, UK. Atmos. Chem. Phys. 15, 10107–10125.

Bernardoni, V., Vecchi, R., Valli, G., Piazzalunga, A., Fermo, P., 2011. PM10 source apportionment in Milan (Italy) using time-resolved data. Sci. Total Environ. 409, 4788–4795.

Bigi, A., Harrison, R.M., 2010. Analysis of the air pollution climate at a central urban background site. Atmos. Environ. 44, 2004–2012.

Bohnenstengel, S.I., Belcher, S.E., Aiken, A., Allan, J.D., Allen, G., Bacak, A., Bannan, T.J., Barlow, J.F., Beddows, D.C.S., Bloss, W.J., Booth, A.M., Chemel, C., Coceal, O., Di Marco, C.F., Dubey, M.K., Faloon, K.H., Fleming, Z.L., Furger, M., Gietl, J.K., Graves, R.R., Green, D.C., Grimmond, C.S.B., Halios, C.H., Hamilton, J.F., Harrison, R.M., Heal, M.R., Heard, D.E., Helfter, C., Herndon, S.C., Holmes, R.E., Hopkins, J.R., Jones, A.M., Kelly, F.J., Kotthaus, S., Langford, B., Lee, J.D., Leigh, R.J., Lewis, A.C., Lidster, R.T., Lopez-Hilfiker, F.D., McQuaid, J.B., Mohr, C., Monks, P.S., Nemitz, E., Ng, N.L., Percival, C.J., Prévôt, A.S.H., Ricketts, H.M.A., Sokhi, R., Stone, D., Thornton, J.A., Tremper, A.H., Valach, A.C., Visser, S., Whalley, L.K., Williams, L.R., Xu, L., Young, D.E., Zotter, P., 2015. Meteorology, air quality, and

health in London: the ClearfLo project. Bull. Am. Meteorological Soc. 779–804.
Brook, R.D., Rajagopalan, S., Pope III, C.A., Brook, J.R., Bhatnagar, A., Diez-Roux, A.V., Holguin, F., Hong, Y., Luepker, R.V., Mittleman, M.A., Peters, A., Siscovick, D., Smith Jr., S.C., Whitsel, L., Kaufman, J.D., on behalf of the American Heart Association Council on Epidemiology and Prevention, Council on the Kidney in Cardiovascular Disease, and Council on Nutrition, Physical Activity and Metabolism, 2010. Particulate matter air pollution and cardiovascular disease: an update to the scientific statement from the american heart association. Circulation 121, 2331–2378.
Carslaw, D.C., 2013. The Openair Manual—Open-source Tools for Analysing Air Pollution Data. King's College London.
Carslaw, D.C., Ropkins, K., 2012. Openair—an R package for air quality data analysis. Environ. Model. Softw. 27–28, 52–61.
Charron, A., Degrendele, C., Laongsri, B., Harrison, R.M., 2013. Receptor modelling of secondary and carbonaceous particulate matter at a southern UK site. Atmos. Chem. Phys. 13, 1879–1894.
Charron, A., Harrison, R.M., Quincey, P., 2007. What are the sources and conditions responsible for exceedences of the 24 h PM_{10} limit value (50 $\mu g\ m^{-3}$) at a heavily trafficked London Site? Atmos. Environ. 41, 1960–1975.
Chow, J.C., Watson, J.G., Lowenthal, D.H., Chen, L.W.A., Zielinska, B., Mazzoleni, L.R., Magliano, K.L., 2007. Evaluation of organic markers for chemical mass balance source apportionment at the Fresno Supersite. Atmos. Chem. Phys. 7, 1741–1754.
Cohen, A.J., Ross Anderson, H., Ostro, B., Pandey, K.D., Krzyzanowski, M., Künzli, N., Gutschmidt, K., Pope, A., Romieu, I., Samet, J.M., Smith, K., 2005. The global burden of disease due to outdoor air pollution. J. Toxicol. Environ. Health Part A 68, 1301–1307.
Crespo, J., Yubero, E., Nicolás, J.F., Lucarelli, F., Nava, S., Chiari, M., Calzolai, G., 2012. High-time resolution and size-segregated elemental composition in high-intensity pyrotechnic exposures. J. Hazard. Mater. 241, 82–91.
Crilley, L.R., Bloss, W.J., Yin, J., Beddows, D.C.S., Harrison, R.M., Allan, J.D., Young, D.E., Flynn, M., Williams, P., Zotter, P., Prevot, A.S.H., Heal, M.R., Barlow, J.F., Halios, C.H., Lee, J.D., Szidat, S., Mohr, C., 2015. Sources and contributions of wood smoke during winter in London: assessing local and regional influences. Atmos. Chem. Phys. 15, 3149–3171.
D'Alessandro, A., Lucarelli, F., Mando, P., Marcazzan, G., Nava, S., Prati, P., Valli, G., Vecchi, R., Zucchiatti, A., 2003. Hourly elemental composition and sources identification of fine and coarse PM10 particulate matter in four Italian towns. J. Aerosol Sci. 34, 243–259.
Dall'Osto, M., Querol, X., Amato, F., Karanasiou, A., Lucarelli, F., Nava, S., Calzolai, G., Chiari, M., 2013. Hourly elemental concentrations in PM2.5 aerosols sampled simultaneously at urban background and road site during SAPUSS – diurnal variations and PMF receptor modelling. Atmos. Chem. Phys. 13, 4375–4392.
Gao, J., Peng, X., Chen, G., Xu, J., Shi, G., Zhang, Y., Feng, Y., 2016. Insights into the chemical characterization and sources of PM2.5 in Beijing at a 1-h time resolution. Sci. Total Environ. 542, 162–171.
Handler, M., Puls, C., Zbiral, J., Marr, I., Puxbaum, H., Limbeck, A., 2008. Size and composition of particulate emissions from motor vehicles in the Kaisermühlen-Tunnel, Vienna. Atmos. Environ. 42, 2173–2186.
Harrison, R.M., Yin, J., Mark, D., Stedman, J., Appleby, R.S., Booker, J., Moorcroft, S., 2001. Studies of the coarse particle (2.5–10μm) component in UK urban atmospheres. Atmos. Environ. 35, 3667–3679.
Harrison, R.M., Dall'Osto, M., Beddows, D.C.S., Thorpe, A.J., Bloss, W.J., Allan, J.D., Coe, H., Dorsey, J.R., Gallagher, M., Martin, C., Whitehead, J., Williams, P.I., Jones, R.L., Langridge, J.M., Benton, A.K., Ball, S.M., Langford, B., Hewitt, C.N., Davison, B., Martin, D., Petersson, K., Henshaw, S.J., White, I.R., Shallcross, D.E., Barlow, J.F., Dunbar, T., Davies, F., Nemitz, E., Phillips, G.J., Helfter, C., Di Marco, C.F., Smith, S., 2012a. Atmospheric chemistry and physics in the atmosphere of a developed megacity (London): an overview of the REPARTEE experiment and its conclusions. Atmos. Phys. Chem. 12, 3065–3114.
Harrison, R.M., Beddows, D.C.S., Hu, L., Yin, J., 2012b. Comparison of methods for evaluation of wood smoke and estimation of UK ambient concentrations. Atmos. Chem. Phys. 12, 8271–8283.
Heal, M.R., Kumar, P., Harrison, R.M., 2012. Particles, air quality, policy and health. Chem. Soc. Rev. 41, 6606–6630.
Kampa, M., Castanas, E., 2008. Human health effects of air pollution. Environ. Pollut. 151, 362–367.
Li, W.J., Shao, L.Y., 2009. Observation of nitrate coatings on atmospheric mineral dust particles. Atmos. Chem. Phys. 9, 1863–1871.
Lucarelli, F., Calzolai, G., Chiari, M., Giannoni, M., Mochi, D., Nava, S., Carraresi, L., 2014. The upgraded external-beam PIXE/PIGE set-up at LABEC for very fast measurements on aerosol samples. Nucl. Instrum. Methods Phys. Res. Sect. B Beam Interact. Mater. Atoms 318, 55–59.
Maxwell, J., Teesdale, W., Campbell, J., 1995. The Guelph PIXE software package II. Nucl. Instrum. Methods Phys. Res. Sect. B Beam Interact. Mater. Atoms 95, 407–421.
Minguillón, M.C., Querol, X., Baltensperger, U., Prévôt, A.S.H., 2012. Fine and coarse PM composition and sources in rural and urban sites in Switzerland: local or regional pollution? Sci. Total Environ. 427–428, 191–202.
Moreno, T., Karanasiou, A., Amato, F., Lucarelli, F., Nava, S., Calzolai, G., Chiari, M., Coz, E., Artíñano, B., Lumbreras, J., Borge, R., Boldo, E., Linares, C., Alastuey, A., Querol, X., Gibbons, W., 2013. Daily and hourly sourcing of metallic and mineral dust in urban air contaminated by traffic and coal-burning emissions. Atmos. Environ. 68, 33–44.
Moreno, T., Querol, X., Alastuey, A., Reche, C., Cusack, M., Amato, F., Pandolfi, M., Pey, J., Richard, A., Prévôt, A.S.H., Furger, M., Gibbons, W., 2011. Variations in time and space of trace metal aerosol concentrations in urban areas and their surroundings. Atmos. Chem. Phys. 11, 9415–9430.
Moreno, T., Querol, X., Alastuey, A., de la Rosa, J., Sánchez de la Campa, A.M., Minguillón, M., Pandolfi, M., González-Castanedo, Y., Monfort, E., Gibbons, W., 2010. Variations in vanadium, nickel and lanthanide element concentrations in urban air. Sci. Total Environ. 408, 4569–4579.
Ning, Z., Polidori, A., Schauer, J.J., Sioutas, C., 2008. Emission factors of PM species based on freeway measurements and comparison with tunnel and dynamometer studies. Atmos. Environ. 42, 3099–3114.
Paatero, P., Tapper, U., 1994. Positive matrix factorization: a non-negative factor model with optimal utilization of error estimates of data values. Environmetrics 5, 111–126.
Paatero, P., 2000. User's Guide for Positive Matrix Factorization Programs PMF2 and PMF3 Part 2. Reference. prepared by University of Helsinki, Helsinki, Finland.
Paatero, P., Hopke, P.K., Song, X., Ramadan, Z., 2002. Understanding and controlling rotations in factor analytic models. Chemom. Intell. Lab. Syst. 60, 253–264.
Paatero, P., Hopke, P.K., 2003. Discarding or downweighting high-noise variables in factor analytic models. Anal. Chim. Acta 490, 277–289.
Pant, P., Harrison, R.M., 2013. Estimation of the contribution of road traffic emissions to particulate matter concentrations from field measurements: a review. Atmos. Environ. 77, 78–97.
Pant, P., Yin, J., Harrison, R.M., 2014. Sensitivity of a chemical mass balance model to different molecular marker traffic source profiles. Atmos. Environ. 82, 238–249.
Polissar, A.V., Hopke, P.K., Paatero, P., Malm, W.C., Sisler, J.F., 1998. Atmospheric aerosol over Alaska: 2. Elemental composition and sources. J. Geophys. Res. Atmos. 103, 19045–19057.
Pope, I.C., Burnett, R.T., Thun, M.J., et al., 2002. LUng cancer, cardiopulmonary mortality, and long-term exposure to fine particulate air pollution. JAMA 287, 1132–1141.
Querol, X., Alastuey, A., Ruiz, C.R., Artiñano, B., Hansson, H.C., Harrison, R.M., Buringh, E., ten Brink, H.M., Lutz, M., Bruckmann, P., Straehl, P., Schneider, J., 2004. Speciation and origin of PM10 and PM2.5 in selected European cities. Atmos. Environ. 38, 6547–6555.
Richard, A., Gianini, M.F.D., Mohr, C., Furger, M., Bukowiecki, N., Minguillón, M.C., Lienemann, P., Flechsig, U., Appel, K., DeCarlo, P.F., Heringa, M.F., Chirico, R., Baltensperger, U., Prévôt, A.S.H., 2011. Source apportionment of size and time resolved trace elements and organic aerosols from an urban courtyard site in Switzerland. Atmos. Chem. Phys. 11, 8945–8963.
Seinfeld, J.H., Pandis, S.N., 1998. Atmospheric Chemistry and Physics. Wiley.
Singh, H.B., 1995. Composition, Chemistry and Climate of the Atmosphere. Van Nostrand Reinhold, New York.
Taylor, S.R., 1964. Abundance of chemical elements in the continental crust: a new table. Geochim. Cosmochim. Acta 28, 1273–1285.
Thorpe, A., Harrison, R.M., 2008. Sources and properties of non-exhaust particulate matter from road traffic: a review. Sci. Total Environ. 400, 270–282.
Usher, C.R., Michel, A.E., Grassian, V.H., 2003. Reactions on mineral dust. Chem. Rev. 103, 4883–4940.
Vecchi, R., Bernardoni, V., Fermo, P., Lucarelli, F., Mazzei, F., Nava, S., Prati, P., Piazzalunga, A., Valli, G., 2009. 4-hours resolution data to study PM10 in a "hot spot" area in Europe. Environ. Monit. Assess. 154, 283–300.
Viana, M., Kuhlbusch, T.A.J., Querol, X., Alastuey, A., Harrison, R.M., Hopke, P.K., Winiwarter, W., Vallius, M., Szidat, S., Prévôt, A.S.H., Hueglin, C., Bloemen, H., Wåhlin, P., Vecchi, R., Miranda, A.I., Kasper-Giebl, A., Maenhaut, W., Hitzenberger, R., 2008. Source apportionment of particulate matter in Europe: a review of methods and results. J. Aerosol Sci. 39, 827–849.
Visser, S., Slowik, J.G., Furger, M., Zotter, P., Bukowiecki, N., Canonaco, F., Flechsig, U., Appel, K., Green, D.C., Tremper, A.H., Young, D.E., Williams, P.I., Allan, J.D., Coe, H., Williams, L.R., Mohr, C., Xu, L., Ng, N.L., Nemitz, E., Barlow, J.F., Halios, C.H., Fleming, Z.L., Baltensperger, U., Prévôt, A.S.H., 2015a. Advanced source apportionment of size-resolved trace elements at multiple sites in London during winter. Atmos. Chem. Phys. Discuss. 15, 14733–14781.
Visser, S., Slowik, J.G., Furger, M., Zotter, P., Bukowiecki, N., Dressler, R., Flechsig, U., Appel, K., Green, D.C., Tremper, A.H., Young, D.E., Williams, P.I., Allan, J.D., Herndon, S.C., Williams, L.R., Mohr, C., Xu, L., Ng, N.L., Detournay, A., Barlow, J.F., Halios, C.H., Fleming, Z.L., Baltensperger, U., Prévôt, A.S.H., 2015b. Kerb and urban increment of highly time-resolved trace elements in PM10, PM2.5 and PM1.0 winter aerosol in London during ClearfLo 2012. Atmos. Chem. Phys. 15, 2367–2386.
Widory, D., Liu, X., Dong, S., 2010. Isotopes as tracers of sources of lead and strontium in aerosols (TSP & PM2.5) in Beijing. Atmos. Environ. 44, 3679–3687.
Yin, J., Cumberland, S.A., Harrison, R.M., Allan, J., Young, D.E., Williams, P.I., Coe, H., 2015. Receptor modelling of fine particles in southern England using CMB including comparison with AMS-PMF factors. Atmos. Chem. Phys. 15, 2139–2158.
Young, D.E., Allan, J.D., Williams, P.I., Green, D.C., Flynn, M.J., Harrison, R.M., Yin, J., Gallagher, M.W., Coe, H., 2015a. Investigating the annual behaviour of submicron secondary inorganic and organic aerosols in London. Atmos. Chem. Phys. 15, 6351–6366.
Young, D.E., Allan, J.D., Williams, P.I., Green, D.C., Harrison, R.M., Yin, J., Flynn, M.J., Gallagher, M.W., Coe, H., 2015b. Investigating a two-component model of solid fuel organic aerosol in London: processes, PM1 contributions, and seasonality. Atmos. Chem. Phys. 15, 2429–2443.